

# Geometric and electronic structure of commensurate $4\text{Ar}/\text{Ag}(111)-(\sqrt{7}\times\sqrt{7})R19.1^\circ$ by density functional theory

Shizhong Yang and James M. Phillips

*Physics Department, University of Missouri–Kansas City, Kansas City, Missouri 64110, USA*

(Received 17 August 2006; revised manuscript received 23 February 2007; published 6 June 2007)

We report the optimization of a  $4\text{Ar}/\text{Ag}(111)-(\sqrt{7}\times\sqrt{7})R19.1^\circ$  monolayer using first-principles density functional theory. The adsorption energies resulting from our ground-state minimizations are similar for all three anchor sites. A commensurate adsorbate cell is comprised of four argon atoms which settle into three different configurations. We refer to these sites as top, threefold hcp hollow, and threefold fcc hollow sites. Each of these structures has one Ar atom located at one of the base sites of the Ag(111) surface. The remaining three Ar atoms are found near the bridge sites of the silver surface. In both of the hollow site structures, the bridge locations are measurably off of the exact geometric bridge positions while maintaining the  $\sqrt{7}R19.1^\circ$  unit cell. Our results show that both the hcp and fcc hollow sites have slightly lower adsorption energies than the top site, by only 1.5 and 4.5 meV, respectively (per cell of four Ar atoms). The vertical harmonic vibration frequencies were computed for the top, hcp, and fcc hollow sites. They measured 5.22, 5.01, and 5.21 meV, respectively. We studied the possible cause for this high-order commensurate monolayer. We have concluded that neither steric repulsion nor hybridization of the electrons of the Ar atoms is the reason for the commensurability in our model. We propose that the causal mechanism is the Novaco-McTague [Phys. Rev. Lett. **38**, 1286 (1977)] theory for orientational epitaxy.

DOI: [10.1103/PhysRevB.75.235408](https://doi.org/10.1103/PhysRevB.75.235408)

PACS number(s): 71.15.Mb, 71.15.Ap, 68.47.De

## I. INTRODUCTION

Caragiu *et al.*<sup>1</sup> found a commensurate system of  $4\text{Ar}/\text{Ag}(111)-(\sqrt{7}\times\sqrt{7})R19.1^\circ$ . They report that the adsorbate unit cell has one Ar atom located on top of a Ag atom and the other three are on bridge sites (see Figs. 1 and 2). Early experiments by Unguris *et al.*<sup>2</sup> and Gibson and Sibener<sup>3</sup> found that Ar is incommensurate with the Ag(111) surface and that the monolayer is aligned with the step edges found in the Ag(111) surface. The recent experiment<sup>1</sup> found the commensurate structure only by first preadsorbing CO on the Ag(111), thereby nullifying the alignment of the adsorbate to the step edges of the Ag(111) surface.

Bruch<sup>4</sup> has recently performed a classical analysis for the unique commensurate adsorption of the higher-order  $4\text{Ar}/\text{Ag}(111)$  using a special case of Novaco-McTague<sup>5</sup> perturbation theory for orientational epitaxy. Although his calculation does not determine a preference for the low- or high-coordination site to be the anchor for the  $4\text{Ar}$  surface unit cell, it appears to be causal for rotation and spacing.

We attempt to find, by density functional theory, the adsorption site minima and to resolve the physical reasons for the observation of this unique structure. We have organized our paper as follows. Section II introduces the calculation methods we used on the commensurate Ar/Ag(111) models. Section III gives the results of our minimizations of the geometric and electronic structures from our first-principles calculations. Section IV reports the conclusions of our study.

## II. COMPUTATIONAL METHODS

We use first-principles plane-wave density functional theory with the projector augmented wave (PAW) method<sup>6–12</sup> in performing our calculations. The local-density approximation (LDA) rather than the generalized gradient approxima-

tion (GGA) was used in our study. Our calculations use the Vienna *ab initio* simulation package (VASP).<sup>6–11</sup> Earlier investigations on physisorbed systems<sup>13–15</sup> have shown that in some systems LDA may give accurate bond lengths and reasonable adsorption energies. We have opted for LDA. However, one must test for the more appropriate approximation for a particular physical model. For our model, we found that the GGA approach for physisorption on metal substrates has given an overestimation of bond lengths and smaller adsorption energies.

The valence electrons were assumed to be the  $4d$  and  $5s$  electrons for the Ag atoms. In the case of argon atoms, the  $3s$  and  $3p$  electrons were selected as the valence levels. The remaining core electrons were kept frozen.

To compensate for the charge asymmetry found between the two sides of our slab, we added vertical dipole corrections.<sup>16,17</sup> For dipole and quadrupole corrections added to the top and bottom faces of our slab, we placed charge units which gave an additional energy to the top face of our model  $\delta E$  (dipole+quadrupole) =  $-1.103$  meV and a dipole moment  $\delta\mu = -0.133 e\text{\AA}$ . These values were typical for all of the other configurations. These corrections are so small that they could just as well be ignored.

Our unit cell includes six atomic layers of Ag, each layer with seven atoms (see Figs. 1 and 2). The vacuum height between slabs was taken to be  $15 \text{\AA}$ , which was sufficiently large to allow us to ignore the effects from neighboring slab interactions.

It was necessary to carefully test a computation for bulk Ag. Our Ag cubic unit cell contains four Ag atoms. Using a  $17\times 17\times 17$  Monkhorst grid and 350 eV plane-wave energy cutoff, the total energy converged to be less than 1 meV between consecutive iterations. The Ag lattice constant from this calculation is  $d=2.84 \text{\AA}$ , in good agreement with other computations and with an experimental value of  $2.89 \text{\AA}$

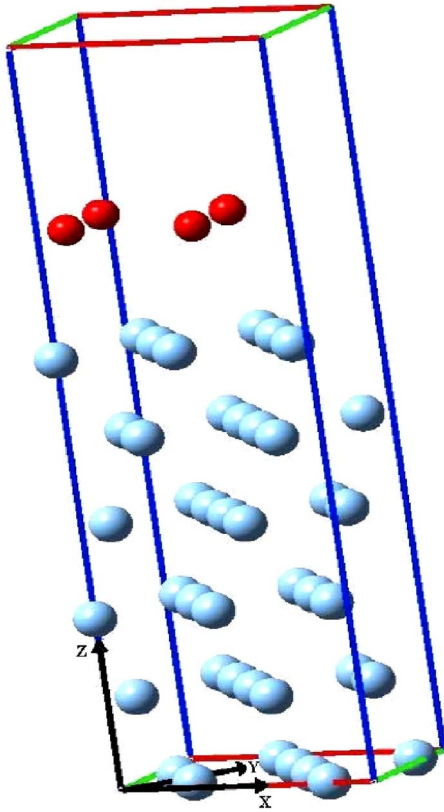


FIG. 1. (Color online) The side view of fcc hollow site Ag(111)- $(\sqrt{7} \times \sqrt{7})R19.1^\circ$ -4Ar unit cell. The darker sphere stands for Ar atoms, while the lighter sphere stands for Ag atoms. The vacuum height is about 15 Å. (The vacuum height was reduced in the figure to save space.)

(Ref. 18 and references therein). In our subsequent calculations for the bare Ag(111) surface, we used a  $7 \times 7 \times 1$  Monkhorst grid and 350 eV plane-wave energy cutoff. Our calculations on the top, hcp hollow, and fcc hollow site structures were based on the equivalent Ag(111) substrates.

The  $k$  space sampling uses a  $7 \times 7 \times 1$  Monkhorst grid in all of our Ar/Ag(111) calculations, electronic energy convergence was set to  $10^{-7}$  eV, and the residual force was set to 1 meV/Å. The coordinates of the bottom four layers of Ag atoms were fixed at their bulk crystal positions, while the upper two layers of Ag atoms and the four Ar atoms (adsorbate) were relaxed. The stability of each surface structure was evaluated by calculating the corresponding adsorption energy per Ar atom:

$$E_{\text{ad}} = [E_{4\text{Ar-Ag}(111)} - E_{\text{Ag}(111)} - N_{\text{Ar}}E_{\text{Ar}}]/4, \quad (1)$$

where  $E_{4\text{Ar-Ag}(111)}$  is the total energy of complex 4Ar/Ag(111),  $N_{\text{Ar}}$  is the number of Ar atoms (4),  $E_{\text{Ag}(111)}$  is the total energy of corresponding slabs, and  $E_{\text{Ar}}$  is the total energy of a single Ar atom.

We have not included an additional van der Waals correction to our density functional approach. We tested our pseudopotentials and our methodology on a bulk Ar crystal. For our Ar bulk calculation, we find the PAW LDA lattice constant to be 4.90 Å (0 K), which is 7.7% lower than the

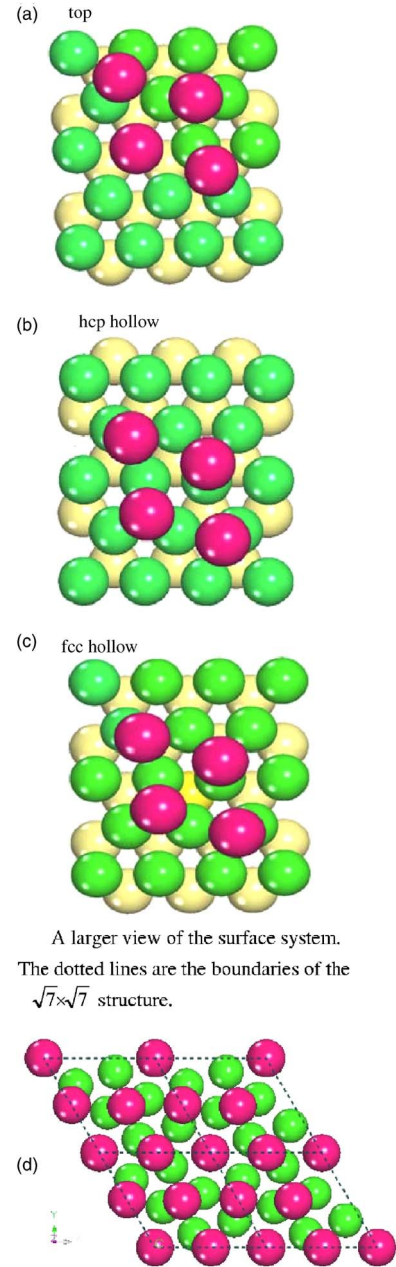


FIG. 2. (Color online) A graphic view of the three base structures: (a) top, (b) hcp hollow, and (c) fcc hollow. The darker spheres represent the Ar atoms, the lighter spheres represent the surface layer silver atoms, while the lightest sphere represents the second layer Ag atoms. (d) A larger view of four  $\sqrt{7} \times \sqrt{7}$  cells of the surface system. The dotted lines are the boundaries of the structure.

experimental value of 5.31 Å (4 K).<sup>1</sup> The PAW Perdew-Burke-Ernzerhof (GGA) lattice constant is 5.71 Å (0 K), which is 7.5% higher than the experimental value. It would appear that such an omission would be an ambiguous correction to the change in energy.

### III. RESULTS AND DISCUSSIONS

Before the adsorption calculation, we did a Ag(111) substrate relaxation. The bottom four layers of Ag atoms were

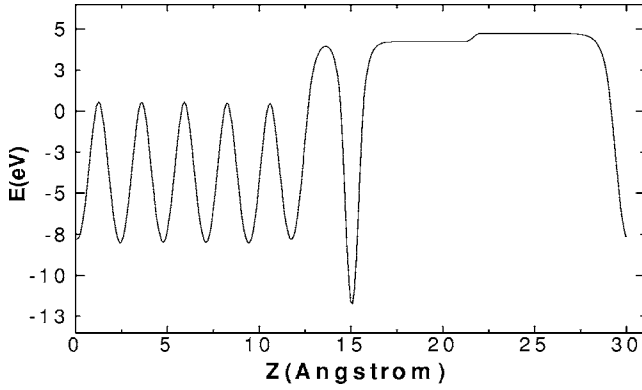


FIG. 3. The average potential along the vertical direction of the fcc hollow structure. The Fermi level is  $-0.15$  eV in the scale of the figure.

fixed at their bulk atom positions, while the first two layers of Ag atoms were fully relaxed. The first two surface layers of Ag have been vertically contracted by  $\Delta d_{12}=0.43\%$  and  $\Delta d_{23}=0.13\%$ , respectively. This is smaller than an earlier calculation which found the first layer Ag to be contracted by 1.4%.<sup>18</sup>

We applied a Bader charge analysis,<sup>19</sup> which showed that a surface atom has a charge  $-0.0222|e|$ , while a second layer atom has a positive charge computed to be  $0.0213|e|$ . These charges are within the same range and of the same sign as those from a single Ar on Ag(111) in a recent cluster calculation.<sup>20</sup> These small values indicate that chemical bonding does not contribute significantly to the resulting configurations.

We obtain a value for the work function and its change upon adsorption. Using density functional theory, we compute the electronic potential across the silver slab, the adsorbed argon atom, and the vacuum (see Fig. 3). The average potential along the vertical direction of fcc hollow structure is given in Fig. 3, which shows that the effective potential in the vacuum near the surface has dropped to a lower value. Note that in Fig. 3 the Fermi energy is  $-0.15$  eV. The other two configurations, top and hcp sites, have very similar curves. The potential difference just outside the argon adsorbate to the potential on the back side of our slab is taken as a measure of the work function.<sup>14</sup> Our calculated Ag(111) work function is 4.89 eV, which is in fair agreement with the experimental value of 4.75 eV (Ref. 21) (see Fig. 3). In Table I, we show our results for the changes in the work function for the different adsorption sites. Our results show, for the fcc hollow position, the difference between before and after the adsorption to be 0.5 eV, and for both the top and hcp hollow sites the differences are 0.49 eV. For comparison, a recent experiment by Hückstädt *et al.*<sup>22</sup> using a Kelvin probe measures the work function difference to be 0.40 eV for Ar/Ag.

The results from our  $4\text{Ar}/\text{Ag}(111)-(\sqrt{7}\times\sqrt{7})R19.1^\circ$  calculations for the geometric and electronic values are summarized in Table I. The adsorption energies per Ar atom for the three adsorption minima were found in the following order:  $E_{\text{ad}}(\text{top}) > E_{\text{ad}}(\text{hcp}) > E_{\text{ad}}(\text{fcc})$  with the values of  $-130.82$ ,  $-131.21$ , and  $-131.93$  meV, respectively. Our results pro-

TABLE I. The calculated results for commensurate Ar/Ag(111).  $\Delta W$  (eV) is the change of work function before and after the Ar adsorption on Ag(111) surface.  $E_{\text{ad}}$  (meV) is the adsorption energy.  $d_{\text{Ar-Ag}}$  is the vertical distance from Ar adsorbate to the Ag(111) surface.  $\Delta d_{\text{Ar}}$  ( $\text{\AA}$ ) is the height difference between the on-site Ar and the three bridge site Ar atoms.  $\Delta d_{\text{Ag}}$  ( $\text{\AA}$ ) is the height difference between the base site Ag and the three off-site Ag atoms. [(+) stands for higher while (−) stands for lower].  $Q_{\text{Ar}}$  is the Bader charge for each Ar atom.  $Q_{\text{Ag1}}$  is the average Bader charge of the first layer surface Ag atoms.  $Q_{\text{Ag2}}$  is the Bader charge for the second layer surface Ag atoms. (The charge unit is  $|e|$ .) The harmonic frequency for vertical vibration of Ar is  $\nu_{\text{Ar}}$  in meV.

	Top	hcp hollow	fcc hollow	Expt.
$E_{\text{ad}}$	130.82	131.21	131.93	$99 \pm 7^{\text{a}}$
$\Delta W$	0.49	0.49	0.50	$0.40^{\text{b}}$
$d_{\text{Ar-Ag}}$	3.29	3.30	3.29	$3.22 \pm 0.072^{\text{a}}$
$\Delta d_{\text{Ar}}$	+0.025	+0.01–0.03	< 0.01	$0.01 \pm 0.06^{\text{a}}$
$\Delta d_{\text{Ag}}$	+0.01	< 0.01	< 0.01	$0.06 \pm 0.08^{\text{a}}$
$Q_{\text{Ar}}$	0.0189	0.0193	0.0194	NA
$Q_{\text{Ag1}}$	−0.0118	−0.0111	−0.0114	NA
$Q_{\text{Ag2}}$	+0.0222	+0.0208	+0.0212	NA
$\nu_{\text{Ar}}$	5.22	5.01	5.21	$3.67^{\text{c}}$

<sup>a</sup>Reference 2.

<sup>b</sup>Reference 22.

<sup>c</sup>Reference 3.

duce a deeper potential than in an earlier computation.<sup>20</sup> When compared with those from a DFT-LDA cluster calculation,<sup>20</sup> Kirchner *et al.* found the adsorption energy to be  $-100$  meV and the experimental value of  $99 \pm 7$  meV in Ref. 2. This result is closer to the experiment than ours. However, it has been shown that cluster models have an insufficient work function to be reliable on adsorption energies while giving good results on local properties. We have made a broad review of the existing literature on cluster calculations. It appears that the results of adsorption energy calculations vary widely depending on the type of bonding involved and, most importantly, the number of atoms in the cluster. As Kirchner found, one size cluster gives one adsorption site and another size gives a different one. Our review found that some systems differ from experiment by a factor of 4 in the adsorption energy when done by a cluster calculation. Some other systems with certain types of bonding and with a certain number of atoms in the cluster may appear to be close to experiment. In our assessment, Kirchner's height of the adsorbate is a good number and the adsorption energy is a bit of good fortune. Also, the computation<sup>20</sup> is at the ground state and the experiment is not.

In the case of the top site, we found the average distance between Ar and the Ag(111) surface to be 3.29  $\text{\AA}$ . This result is in reasonable agreement with experimental data, which measure  $3.22 \pm 0.07$   $\text{\AA}$ .<sup>1</sup> The height of a top site Ar is found to be 0.025  $\text{\AA}$  higher than the three bridge site Ar atoms, while the height of Ag atom right under the top Ar atom is 0.01  $\text{\AA}$  higher than the other surface Ag atoms.

In the case of the threefold hcp hollow site, the vertical distance prediction between Ar and the Ag(111) surface is

3.30 Å by our computation. The height of the Ar on the hollow sites varies from 0.01 to 0.03 Å higher than the other three bridge site Ar atoms. For the fcc hollow site, the average distance between Ar and Ag(111) surface is 3.29 Å. These vertical distances suggest only that our computational accuracy in this model is of the order of 0.01 Å. Neither our computational accuracy nor the experimental measurements of these distances are absolute to this level.

To compute the vertical Ar vibration frequency for each of the three configurations in the monolayer, we optimized the Ar in each of the structures (the top, hcp, and fcc sites). The Ar atoms were displaced a small distance from their corresponding equilibrium positions. The total energies were calculated for each configuration. Using the energy as a function of displacement, we obtained the harmonic approximation by solving one-dimensional Schrödinger equation. We calculated the top, hcp, and fcc harmonic frequencies to be 5.22, 5.01, and 5.21 meV, respectively. The experimental frequencies are known from the data taken by the Gibson-Sibener<sup>3</sup> inelastic helium scattering experiment. They measured the vertical vibrations to be 3.67 meV. The discrepancy between the calculated frequencies and the experimental one ranges from 37% to 42%. The temperature in the experiment was 22 K, whereas in our computations, the temperature was assumed to be 0 K. Note that the experiment was done on an incommensurate monolayer. The LDA that we used in our calculations would appear to overestimate the frequencies. However, ours are consistent with the frequencies computed in this manner by Da Silva *et al.*<sup>13,14</sup>

The lateral interaction energies were calculated by adding Ar atoms one by one onto the unit cell in their optimized positions. For the three structures, our results for the lateral energies were  $E_{\text{top}} = -63.35$  meV,  $E_{\text{hcp}} = -63.42$  meV, and  $E_{\text{fcc}} = -63.42$  meV, respectively. These results are reasonable when compared to a recent calculation of the Xe-Xe lateral interaction in  $(\sqrt{3} \times \sqrt{3})R30^\circ$  Xe/Pt(111),<sup>23</sup> which was  $-59$  meV. Our three lateral argon energies have similar values to the commensurate Xe structure. At first sight, this comparison may appear unusual. However, the pair separations for both of these commensurate structures are far from their close-packed distances. In these registered structures, the pair separations measure (Ar  $\approx 3.67$  Å) and (Xe  $\approx 4.48$  Å). At the commensurate pair separations, the atoms are located high on the attractive side of their potential. The values of the potentials for these two systems are similar at these respective distances.

Our Bader charge analysis of the three optimized structures show that after the Ar adsorption, the surface charge is very slightly negative, as can be seen from the  $Q_{\text{Ag1}}$  in Table I. The second layer average Bader charge  $Q_{\text{Ag2}}$  has a very small positive modification. The Ar atoms also become slightly positive in all of the structures. We conclude that there is essentially little charge transfer in any of the structures. These results show that the very small charge shifts would have little effect in choosing a preferred site between these optimized structures. The Bader charge transfers are so small that their absolute values are all less than  $0.023|e|$ .

### A. Electronic density of states

Figure 4 shows the partial density of states for the adsorbed Ar atom on all of the base sites decomposed into the

$S$ ,  $P_x$ ,  $P_y$ , and  $P_z$  states. We have separately computed the density of states for the Ar atom in each of the top, hcp, and fcc sites (left side of Fig. 4) compared to the other three Ar atoms on the bridge sites (right side of Fig. 4). In all of these graphs, we note that the  $P_x$  and  $P_y$  bands are more expanded in their energy range than that of  $P_z$  by 0.75 eV. The magnitudes of  $P_z$  of all the left side graphs are greater than  $P_x$  and  $P_y$ . The overall magnitude of  $P_z$  for the bridge sites on the right side of Fig. 4 are much greater. The hcp site partial density of state (DOS) graphs are very similar to that of fcc site partial DOS. The distinguishable differences are found in the  $P_z$ 's shape and magnitude. This is true, in a similar way, for all of the basic sites.

It is clear from Fig. 4 that the Ar adsorbate atoms have been hybridized. The states for the  $3s$  and  $3p$  electrons are different from their line energy levels, which we computed for an isolated Ar atom. The density of states is nonzero well below the Fermi level (from  $-5.5$  to  $-6.75$  eV), but not shown in the figures. The small differences in the Ar  $3s$  and  $3p$  DOS between the various base sites (Fig. 4, on left side for the top, hcp hollow, and fcc hollow sites) and the corresponding bridge sites (Fig. 4, right side) indicate little evidence for a particular site preference.

We continued our study of the DOS by considering the  $4d$  and  $5s$  electrons for the individual Ag atoms in the Ag(111) surface. The DOS for the  $5s$  electrons has structure from  $-5.5$  to  $+5.5$  eV, which is consistent with the cluster calculation in Ref. 18. For a single Ag atom found in all three of the surface sites, we find little difference in the DOS for the  $5s$  electrons between any of the adsorption sites. In the neighborhood of the Fermi level, there appears to be nearly identical values in the DOS magnitude and in their distribution. Again, we find little evidence for adsorption site preference. We also compute the DOS for the  $4d$  electrons for the surface Ag atoms: they all fall between  $-7.5$  and  $-2.5$  eV. Panaccione *et al.*<sup>24</sup> published a high-energy photoemission experiment on silver. Our computed density of states for the Ag(111) surface is reasonably consistent with their data on the bulk and to other previous calculations.<sup>25</sup> There is no support in our model for a preference concerning any of the three base site positions. After a number of computations, we are left with an essentially null result for hybridization effects on adsorption site preference. Since there is very little difference between the DOS of the Ag surface sites and since it would require numerous redundant figures, we have omitted them from our paper.

We considered the possibility of Pauli exclusion (steric repulsion) as a cause for site preference in our model, so we computed the Bader charge distributions over the adsorbate and/or substrate structures. In Table I, the Bader charges for the Ar atoms ( $Q_{\text{Ar}}$ ) in the three different base sites are negative and very small, i.e., they are computationally indistinguishable.

In the first layer, the Ag sites have Bader charges that are also negative and very small (Table I,  $Q_{\text{Ag1}}$ ). In the second layer of Ag (see Table I),  $Q_{\text{Ag2}}$  is very small and positive for all sites. The base sites have a very small dipole moment at each adsorption location and they are equal in the limits of

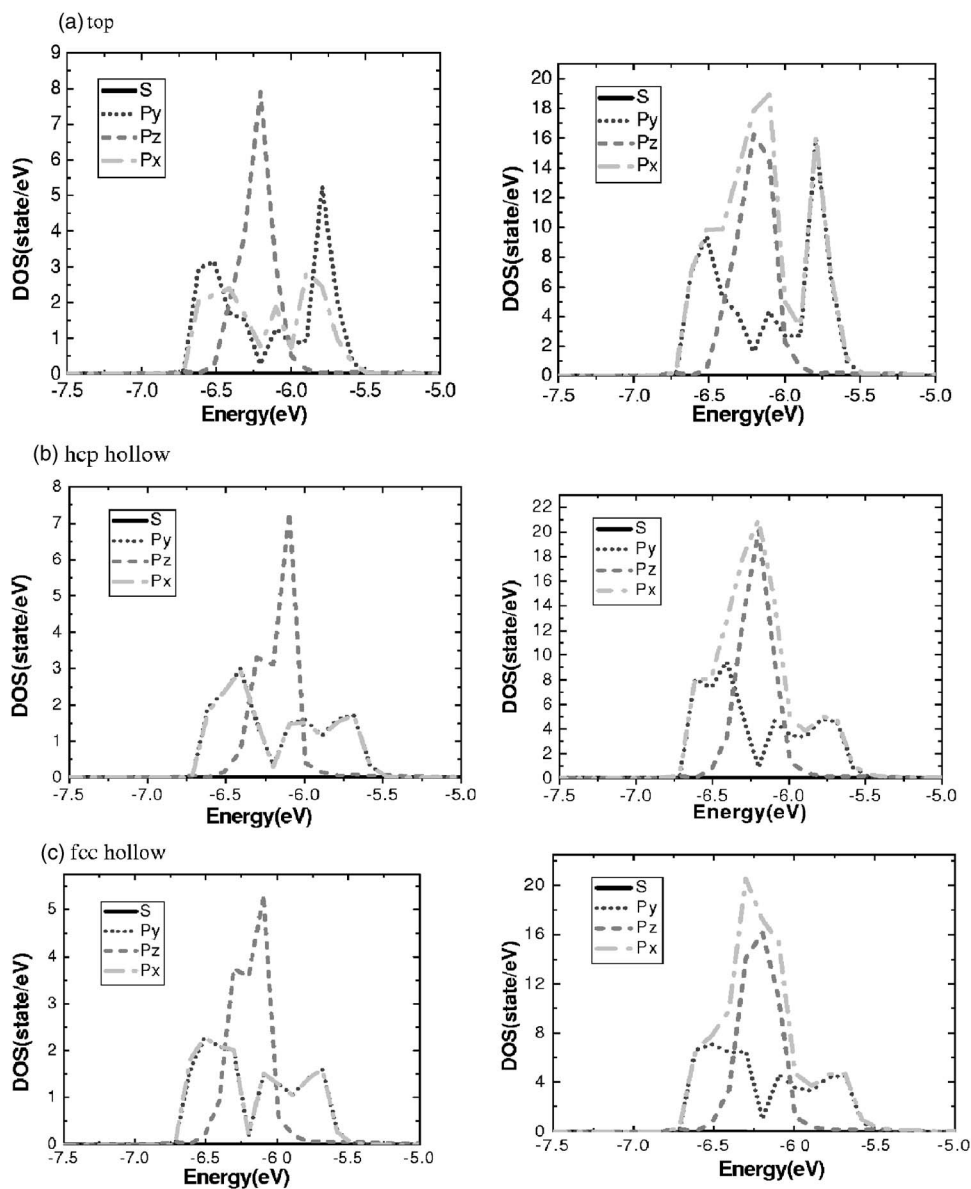


FIG. 4. Partial density of states decomposed into  $S$ ,  $P_x$ ,  $P_y$ , and  $P_z$ . All the left-side graphs are for the base Ar atoms and all the right-side graphs are for the three bridge site Ar atoms: (a) top, (b) hcp hollow, and (c) fcc hollow. The Fermi energy is at zero eV. Note that the  $S$  density of states is zero in the range.

our computations. We find the bridge sites to be weakly attractive when considering the electronic density distribution of the bare Ag(111) surface. Three of the four atoms in each of these commensurate structures fall on bridge sites. Any repulsive effect of the base sites must necessarily be small since all of the geometrically minimized structures have similar adsorption energies. Using the Bader charge analysis for the adsorbate and substrate complex, we conclude that steric repulsion is of little effect in the choice of adsorption site preference.

### B. Comparable commensurate system

We thought it would also be interesting to compute the adsorption energies of another similar commensurate structure, Ru(0001)-(3×3)-4Kr. We found the three base structures (top, fcc, and hcp hollow) minimized to nearly identical values (175 meV). These computational values were equal

up to four significant figures. Experimentally, the adsorption energy for this system was observed to be 152 meV.<sup>26</sup> The experiments of Narloch and Menzel<sup>27</sup> used low-energy electron diffraction (LEED)  $I$ - $V$  techniques at 20 K. They observed the fcc hollow and hcp hollow structures and found them in a compositional ratio of (48%:52%). We calculate the perpendicular distances from the substrate to the adsorbate atoms to be  $d_{\text{top(Kr-Ru)}}=3.352$  Å,  $d_{\text{fcc(Kr-Ru)}}=3.497$  Å (with Kr slightly higher than for the three bridge site Kr atoms by about 0.06 Å), and  $d_{\text{hcp(Kr-Ru)}}=3.540$  Å (with Kr slightly higher than the three bridge site Kr atoms by about 0.08 Å). Experimentally, Narloch and Menzel<sup>27</sup> measured the perpendicular distance from the Kr to the Ru surface to be 3.70 Å. When compared to other rare-gas atoms on metals, this value seems a bit large. Their measured distance is considerably out of sequence with a large body of other adsorption data. Such a difference may make the LEED analysis suspicious. They did not observe the top site structure as proposed by Diehl *et al.*<sup>28</sup>

### C. Novaco-McTague perturbation theory: Orientational epitaxy

Bruch<sup>4</sup> performed a classical calculation on a higher-order orientational commensurability for two-dimensional periodic surface systems with different length scales. He found the minimum energy to be that of the  $4\text{Ar}/\text{Ag}(111)-(\sqrt{7} \times \sqrt{7})R19.1^\circ$  structure using an application of the Novaco-McTague perturbation theory.<sup>5</sup> Bruch analyzed the second-order perturbation energy distortion in the mass density waves for the difference in the parallel and perpendicular polarizations. The frequencies were evaluated at an  $M$  point of the first Brillouin zone for the monolayer. Our computational method does not provide us with a sufficiently accurate perpendicular vibration and we do not find the parallel mode at all using our simple method. Consequently, we are unable to provide a conformation for the perturbation theory study. Bruch's analysis does not conclude which of the possible proposed configurations are the most stable, but he gives a criterion for the necessary accuracy in order to determine the surface corrugation. Bruch<sup>4</sup> suggested that the energy resolution should be within 0.1 meV and the vertical corrugation to be  $\Delta z=0.15 \text{ \AA}$  in order to provide a clear distinction. Our relative computational accuracy between configurations should be sufficient, but our absolute accuracy to the physical system is not.

## IV. CONCLUSIONS

In an attempt to answer how these unusual structures  $\text{Ag}(111)-(\sqrt{7} \times \sqrt{7})R19.1^\circ-4\text{Ar}$  physically occur, we were led to the possibilities of steric repulsion and/or hybridization of Ar in its various positions with the Ag substrate atoms. The steric repulsion is difficult to understand because the three bridge sites appear in all of the models. Our study of the hybridization of the adsorbate and the substrate atoms shows each of the three structures to be similar within a few meV. So we are left without any indication that a particular preference is in order for the three structures. This led us to conclude that the causal mechanism is the Novaco-McTague theory for orientational epitaxy. As studied by Bruch,<sup>4</sup> the

top site versus hollow site question was left to an *ab initio* calculation for the constants of the Steele expansion.<sup>29</sup> In effect, this was to be our calculation. Our results are not sufficient to judge the absolute values of the physical system. As in most computational approaches, they are best evaluated relative to each other.

In comparison with the experiment by Caragiu *et al.*,<sup>1</sup> our computations are in agreement in that we find a clear minimum for the top site. We find this experimentally observed structure for the top site to be a local energy minimum, but we also find two other structures (the hollow sites) to have slightly lower adsorption energy minima. The mystery, to us, is why commensurate islands of  $\text{Ag}(111)-(\sqrt{7} \times \sqrt{7})R19.1^\circ-4\text{Ar}$  of all three structures are not observed. The similar structure observed by Narloch and Menzel<sup>27</sup> on the  $\text{Ru}(0001)-(3 \times 3)-4\text{Kr}$  system found only two of the three structures we computed. Why should there be such conflicting observations between these similar systems? Our computations show that the relative energies are within a few meV in the case of  $\text{Ar}/\text{Ag}(111)$  and identical in the case of  $\text{Kr}/\text{Ru}(111)$ . The relative values from site to site should take in all of the competing interactions in our computations. Since the value of the work function we computed is higher by 0.1 eV, it is possible that our absolute values are higher than the observed adsorption energies, but the choice of base sites should be relatively close to the physical system.

There are a few questions that need to be addressed. How could temperature effects make certain sites preferable? Our calculations are ground-state results at an assumed temperature of 0 K. We note that the Ar experiments are done at 31 K and the Kr experiments are done at 20 K. Does the preadsorption with CO affect the ground-state configuration? Is our computational approach reliable to this geometric precision? Our computational approach seems to be reliable when applied to several other surface systems by ourselves and other authors.<sup>13-15,30-32</sup>

## ACKNOWLEDGMENT

We thank L. W. Bruch and R. D. Diehl for several discussions of our work.

<sup>1</sup>M. Caragiu, G. S. Leatherman, Th. Seyller, and R. D. Diehl, *Surf. Sci.* **475**, 89 (2001).

<sup>2</sup>J. Unguris, L. W. Bruch, E. R. Moog, and M. B. Webb, *Surf. Sci.* **109**, 522 (1981).

<sup>3</sup>K. D. Gibson and S. J. Sibener, *J. Chem. Phys.* **88**, 7862 (1988).

<sup>4</sup>L. W. Bruch, *Phys. Rev. B* **64**, 033407 (2001).

<sup>5</sup>A. D. Novaco and J. P. McTague, *Phys. Rev. Lett.* **38**, 1286 (1977).

<sup>6</sup>G. Kresse and J. Hafner, *Phys. Rev. B* **47**, R558 (1993).

<sup>7</sup>J. Furthmüller, J. Hafner, and G. Kresse, *Phys. Rev. B* **50**, 15606 (1994).

<sup>8</sup>G. Kresse and J. Furthmüller, *Comput. Mater. Sci.* **6**, 15 (1996).

<sup>9</sup>G. Kresse and J. Furthmüller, *Phys. Rev. B* **54**, 11169 (1996).

<sup>10</sup>VASP 2003 Manual, see website: <http://cms.mpi.univie.ac.at/vasp/>

<sup>11</sup>G. Kresse and D. Joubert, *Phys. Rev. B* **59**, 1758 (1999).

<sup>12</sup>P. E. Blöchl, *Phys. Rev. B* **50**, 17953 (1994).

<sup>13</sup>J. L. F. Da Silva, C. Stampfl, and M. Scheffler, *Phys. Rev. Lett.* **90**, 066104 (2003).

<sup>14</sup>J. L. F. Da Silva, C. Stampfl, and M. Scheffler, *Phys. Rev. B* **72**, 075424 (2005).

<sup>15</sup>S. Yang, L. Ouyang, J. M. Phillips, and W. Y. Ching, *Phys. Rev. B* **73**, 165407 (2006).

<sup>16</sup>J. Neugebauer and M. Scheffler, *Phys. Rev. B* **46**, 16067 (1992).

<sup>17</sup>L. Bengtsson, *Phys. Rev. B* **59**, 12301 (1999).

<sup>18</sup>M. Methfessel, D. Hennig, and M. Scheffler, *Phys. Rev. B* **46**, 4816 (1992).

- <sup>19</sup>R. F. W. Bader, *Atoms in Molecules—A Quantum Theory* (Oxford University Press, Oxford, 1990).
- <sup>20</sup>E. J. J. Kirchner, A. W. Kleyn, and E. J. Baerends, *J. Chem. Phys.* **101**, 9155 (1994).
- <sup>21</sup>H. B. Michaelson, *J. Appl. Phys.* **48**, 4729 (1977).
- <sup>22</sup>C. Hückstädt, S. Schmidt, S. Hüfner, F. Forster, F. Reinert, and M. Springborg, *Phys. Rev. B* **73**, 075409 (2006).
- <sup>23</sup>A. E. Betancourt and D. M. Bird, *J. Phys.: Condens. Matter* **12**, 7077 (2000).
- <sup>24</sup>G. Panaccione, G. Cautero, M. Cautero, A. Fondacaro, M. Gioni, P. Lacovig, G. Monaco, F. Offi, G. Paolicelli, M. Sacchi, N. Stojic, G. Stefani, R. Tommasini, and P. Torelli, *J. Phys.: Condens. Matter* **17**, 2671 (2005).
- <sup>25</sup>I. Landau, P. Pianetta, S. Doniach, and F. Spicer, *Nature (London)* **250**, 214 (1974).
- <sup>26</sup>H. Schichting and D. Menzel, *Surf. Sci.* **272**, 27 (1992).
- <sup>27</sup>B. Narloch and D. Menzel, *Surf. Sci.* **412/413**, 562 (1998).
- <sup>28</sup>R. D. Diehl, Th. Seyller, M. Caragiu, G. S. Leatherman, N. Ferralis, K. Pussl, P. Kaukasoina, and M. Lindroos, *J. Phys.: Condens. Matter* **16**, S2839 (2004).
- <sup>29</sup>W. A. Steele, *Surf. Sci.* **36**, 317 (1973).
- <sup>30</sup>S. Yang and J. M. Phillips (unpublished).
- <sup>31</sup>J. E. Müller, *Phys. Rev. Lett.* **65**, 3021 (1990).
- <sup>32</sup>S. Yang, J. M. Phillips, and L. Ouyang, *Phys. Rev. B* **74**, 245424 (2006).